

A crustal deformation model around the Izu Peninsula considering inland faults and elastic collision

*kazuma Mochiduki¹, Yuta Mitsui²

1.Graduate School of Integrated Science and Technology, Shizuoka University, 2.Department of Geoscience, Faculty of Science, Shizuoka University

This study models crustal deformation focusing on inland faults and elastic collision around the base of the Izu Peninsula using GNSS(Global Navigation Satellite System) time-series data. First, in order to extract steady deformation, we correct the F3 solution data about antenna replacement from January., 2000 to January., 2010, and remove non-stationary variations using models of earthquakes, volcanic deformation and slow slip events. Next, we set elastic collisional power sources around the base of the Izu Peninsula, locking of plate boundaries, a deep creep of inland faults and a stationary volcanic deformation with a dislocation model and rotational motion of rigid bodies of the Izu micro plate and the Izu arc block (Nishimura, 2011). Then we perform an inverse analysis for the crustal deformation in this region.

The inversion result exhibits that elastic collisional power sources work at -12.7 mm/yr on the eastern foot of Mt. Hakone, 6.2 mm/yr on the northern foot, 11.6 mm/yr on the western foot and -0.5 mm/yr in the eastern Suruga bay. The plate boundaries are locked at 6 - 43.8 mm/yr beneath the Sagami trough, 3.6 - 39.3 mm/yr beneath the Suruga trough, 10 - 15.9 mm/yr in a southern edge of the Itoigawa Shizuoka Tectonic Line and 11 - 105.5 mm/yr on the boundary between the Izu micro plate and the Izu arc block. The inland faults creep at 23.3 mm/yr in deep extension of the Northern Izu fault zone and 23.4 mm/yr in deep extension of the Sagiriko Rokuroba fault group. In addition, the stationary volcanic deformation source at Mt. Mihara in the Izu-oshima island expands at $2.0 \times 10^6 \text{ m}^3/\text{yr}$. Furthermore, for the Honshu, the Izu micro plate rotates at -3.1 °/Myr with the Euler pole of 36.57 °N, 139.72 °E and the Izu arc block rotates at -11.3 °/Myr with the Euler pole of 34.95 °N, 140.46 °E. The spatial variations of the elastic collisional power sources correspond to actual terrain around the base of the Izu Peninsula.

Keywords: elastic collision, inland fault, plate subduction, volcanic inflation, Izu collisional zone, crustal deformation

Analysis of crustal deformation due to slip across faults using finite element method

*Yoshiaki Ida¹, Aiko Kikuchi¹, Norio Toda¹

1. Advance Soft Co.

In Advance Soft Cooperation a computer program, named FrontSTR/GEOS, has been developed for the calculation of deformation due to fault slips and magma migration using finite element method. This program utilizes for the finite element calculation the program Front/STR that was obtained in the MEXT project "The Research and Development of Innovative Simulation Software" and contains some additional parts that have been developed by us to represent the effects of fault displacements and magma migration. In the finite element calculation displacements at nodal points are usually calculated in an iterative CG method. The program can be executed with a personal computer or a large computer allowing parallel computing.

The mesh for the finite element calculation is generated automatically in the following two steps by the program "meshgen" that has been developed by us. Namely, the region in question is first divided by hexahedron elements to make the whole mesh and then faults are put into the whole mesh. These two steps are independent so that we do not have to remember the whole mesh when we define faults.

The whole mesh consists of one or several blocks. Each block is divided by hexahedron elements whose sizes are constant or change at a constant rate with the location of the element. The surface topography can be taken into account by adjusting the thicknesses of the top elements. The effects of artificial boundaries placed on the sides and floor of the region can be made sufficiently small by introducing infinite elements along the boundaries. Elastic constants of each element can be set consistently with a three-dimensional distribution of seismic velocities.

The fault surfaces are defined by assemblies of triangles or quadrangles. The fault slip is specified at each vertex of the triangles or quadrangles and interpolated into their interiors. There may be more than one faults in the region but they cannot be intersected one another. Furthermore, each fault must stay within one of the blocks.

The elements through which one of the faults passes are further divided by the fault plane into some elements that have additional nodal points on the fault plane. Each of these new nodal points have double displacement values whose difference represents the slip or opening of the fault. In the finite element calculation the double displacement values are calculated with other displacements in the MPC method so as to meet both elastic equilibrium condition and prescribed constraints put on the double displacements.

The basis of our computer program is the calculation of elastic deformation due to prescribed displacement difference across the fault. The relaxation of viscoelastic deformation is traced with time based on the nature that the viscoelastic effect can be represented as an additional external force in the calculation of elastic deformation. The effect of gravity is taken into account in this calculation of relaxation. Some stress conditions on fault planes can be treated by adjusting suitably the constraints on the double displacements.

The program is applied to the deformation due to the fault slip during the great earthquake east off the northern district of Japan, March 11, 2011. The influence of fault geometry and slip distribution on crustal deformation is examined for this event. Relaxation of deformation after the event is evaluated under a suitable assumption of viscosity distribution. The merit in representing fault slip by double displacements is also demonstrated using this event.

Keywords: finite element method, fault slip, the great earthquake east off the northern district of Japan

Interseismic Crustal Deformation in Southwest Japan: Oblique Plate Convergence and Forearc Block Motion

*Masahiko Shiomi¹, Takao Tabei², Takeo Ito³

1.Graduate School of Science, Kochi Univ., 2.Faculty of Science, Kochi Univ., 3.Earthquake and Volcano Research Center, Nagoya Univ.

The Median Tectonic Line (MTL) is the longest arc-parallel strike-slip fault in southwest Japan, whose right-lateral motion originates from oblique subduction of the Philippine Sea plate (PHS) at the Nankai trough. MTL separates the forearc block from the rest of the overriding southwest Japan arc. Rate of relative block motion between them is estimated small enough compared with the dominant crustal shortening in the direction of PHS convergence since the interseismic coupling on the plate interface is generally strong. Nevertheless strain accumulation on the MTL fault plane is very important because it is capable of producing a major inland earthquake in the future. In this study, we simultaneously deal with elastic deformation due to strong coupling on the PHS interface, forearc block motion relative to the southwest Japan arc, and small shear deformation due to partial locking of the shallower part of the MTL fault plane.

We use horizontal and vertical displacement rates derived from GEONET final coordinate time series at 291 sites from Kyushu to Kinki regions during the period of 2004-2009. In addition we incorporate horizontal displacement rates from dense GPS campaign observations at 37 sites deployed along two traverse lines across the MTL. The PHS interface is reproduced by more than 1000 triangular elements from 5 to 60 km in depth. Similarly MTL is divided into four segments from east to west and each segment is modeled by a uniform rectangular plane with a dip angle of 50 degrees. Also the MTL fault plane is assumed to be partially locked from the surface to the depth of 15 km. We introduce Markov Chain Monte Carlo method (MCMC) for simultaneous estimation of parameters. The MCMC derives posterior probability density functions of unknown parameters from enormous forward calculations. These calculations are executed by random value sampling which are generated by Monte Carlo method based on Markov chain algorithm. Even in a case of the model with a large number of unknowns, we can estimate parameter values and confirm their validities. In our modeling, new constraints are introduced that forearc block motion relative to the southwest Japan arc is inherently parallel to the strike of MTL and slip-deficit rate on the MTL fault plane does not exceed the rate of the relative block motion across the MTL.

The results shows that distribution of interseismic slip deficit rates on the PHS interface is very similar to those obtained in several previous studies. The strongest-locked region (> 60 mm/yr) exists at the depth of 15-25 km under Tosa Bay just south of Shikoku, which nearly overlaps the main rupture zone at the last megathrust event in 1946. The rate of the forearc block motion relative to the southwest Japan arc is estimated as about 4 mm/yr westward. Locking of the shallow MTL fault plane shows slight lateral variation from east to west. We find that the eastern segment is nearly fully locked, then the locking weakens toward the west. It is interesting whether the results are related to the difference of strain accumulation rate and recurrence interval between the segments.

Keywords: Markov Chain Monte Carlo method, Median Tectonic Line, Southwest Japan, GPS observation

Tectonic and volcanic deformation at the Azores Triple Junction, observed by continuous and campaign GPS analysis

*Jun Okada¹, João PM. Araújo², Alessandro Bonforte³, Francesco Guglielmino³, Maria FP. Lorenzo², Teresa JL. Ferreira²

1.Meteorological Research Institute - Japan Meteorological Agency, 2.Centro de Informação e Vigilância Sismovulcânica dos Açores (CIVISA), 3.Istituto Nazionale di Geofisica e Vulcanologia, Sezione di Catania

The Azores archipelago is located at the junction where three tectonic plates meet: the Eurasian, Nubian and North American plates. It is an area of intense seismic and volcanic activity (Gaspar *et al.* 2015). The boundary between the North American and the other two plates is well defined, but the boundary between the Eurasian and Nubian plates is obscure. Previous geological, geophysical and geochemical studies have revealed diffuse and complex tectonic regime for this boundary zone. The use of space geodesy techniques, such as Global Positioning System (GPS), has provided important contributions to unveiling these diffusive plate boundary characteristics (Fernandes *et al.* 2004, 2006; Trota 2009; Marques *et al.* 2013) as well as detecting volcanic signals (e.g. Fogo Volcano - Trota 2009). The relation between regional tectonics and local volcanic activity is, however, poorly understood. Few attempts have been made to address the detailed spatial and temporal geodynamic processes. The accumulation of data in recent years at S. Miguel Island, is making such attempts possible.

We analyze 9 continuous GPS (CGPS) stations and the campaign data of the island for the period of 2008-2013 using Bernese5.0 software (Dach *et al.* 2007). In order to tie the estimated coordinates to the global geodetic reference frame - ITRF2005, neighboring international IGS station data are simultaneously processed along with the local datasets. By comparing with the current plate angular velocities (DeMets *et al.* 2010), we find a high-strain-rate (0.28 ppm/yr of expansion) zone in the east of Fogo volcano, which accommodates about 50% of the Eurasian-Nubian plate spreading. Fogo exhibited intense seismic swarm during 2011-2012. The analysis of detrended GPS time-series after subtracting regional plate velocities reveals the existence of two different types of ground deformation associated with the seismicity. One is the edifice-scale inflation of Fogo, which corresponds to the increase in volcano-tectonic events. Another is inflation-deflation reversal in the east of Fogo, which coincides with the sharp decrease in lower-frequency events in August 2012. A strong similarity to the Matsushiro, Japan, earthquake swarm (1965-66) and Campi Flegrei, Italy, volcanic episodes (1969-72 and 1982-85) may suggest importance of the hydrothermal system at Fogo volcano. We propose the following hypothesis for the Fogo unrest: (1) the primary inflation source beneath Fogo promotes lateral diffusion of fluids that is selectively guided by existing cracks/fissures formed from regional extension; (2) an influx of fluids increases pressure in cracks/fissures and generates lower-frequency earthquakes; and (3) discharge of fluids causes pressure decrease and dilatancy recovery (i.e. seismic quiescence). To estimate the source parameters, the result of GPS campaigns is modelled by an integrated inversion using a genetic algorithm. The best fit model agrees well with the regional/local tectonic feature.

Keywords: crustal deformation, GPS, GNSS, plate tectonics, Azores, volcano geodesy

Visco-elastic relaxation in volcano deformation

*Tadashi Yamasaki¹

1.Geological Survey of Japan, AIST

Satellite-based observation (GPS and/or InSAR) has precisely measured surface deformation, but by itself does not derive a mechanism of the deformation. We therefore need to employ some theoretical model in order to understand characteristic deformation pattern for a given source mechanism, only based on which the deformation source mechanism can be objectively deduced from the observation. Magmatic activity in depth is particularly considered as the source mechanism in this study. We employ a parallelized 3-D finite element code, OREGANO_VE [e.g., Yamasaki and Houseman, 2015, *J. Geodyn.*, 88, 80-89], to solve the linear Maxwell visco-elastic response to a given internal inflation/deflation of magma chamber. In a rectangular finite element model domain, the crust is mechanically two-layered, in which an elastic layer with thickness of H is underlain by a visco-elastic layer, but the entire mantle behaves as visco-elastic material. A depth-dependent viscosity (DDV) is adopted for the visco-elastic crust, where the viscosity exponentially decreases with depth due to temperature-dependency: $\eta_c = \eta_0 \exp[c(1 - z/L_0)]$, where η_0 is the viscosity at the bottom of the crust, c is a constant; $c > 0$ for DDV model and $c = 0$ for uniform viscosity (UNV) model, z is the depth, and L_0 is a reference length-scale. The visco-elastic mantle is contrarily assumed to have a spatially uniform viscosity η_m . A sill-like magma chamber is approximated as a spheroid, and its inflation/deflation is implemented by using the split node method developed by Melosh and Raefsky [1981, *Bull. Seism. Soc. Am.*, 71, 1391-1400]. We first employ UNV model with $c = 0$, which shows that visco-elastic relaxation abates the inflation-induced surface uplift with time; The post-inflation subsidence would erase the uplift in $\sim 50 - 100$ times Maxwell relaxation time of the crust unless the inflation occurs within the uppermost elastic layer. The rate of the subsidence is governed by a depth of the inflation and the equatorial radius of the sill; but the latter is not important for the earliest post-inflation period. Time-dependent inflation always accompanies with visco-elastic relaxation, and any significant surface uplift is not expected if the inflation has occurred over the time-scale greater than $\sim 50 - 100$ times crustal relaxation time. DDV model with $c > 0$ is also employed in this study to examine how a spatio-temporal deformation pattern at the surface is deviated from that for UNV model. The predicted model behaviour shows that UNV model behaviour approximates DDV model behaviour, but the apparent UNV which best fits a DDV displacement history depends on distance from the centre of the inflation; smaller viscosities are required at greater distances from the centre of the inflation. Such a model behaviour would expect that the spatio-temporal ground movement also depends on the depth of the sill inflation. Furthermore, a UNV model behaviour that the post-inflation subsidence depends on the thickness of the uppermost elastic layer requires us to examine the DDV model behaviour in terms of an effective elastic thickness for a given DDV structure. The model predictions obtained in this study provide important insights into geodetically detectable ground movement in volcanic provinces.

Keywords: Volcano deformation, Visco-elastic relaxation, Maxwell relaxation time

Crustal deformation by the West Off Satsuma Peninsula earthquake occurred on November 14, 2015

*Shigeru Nakao¹, Hiroshi Yakiwara², Shuichiro Hirano², Kazuhiko Goto², Kazunari Uchida³, Hiroshi Shimizu³

1.Department of Earth and Environmental Sciences, Graduate School of Science and Engineering, Kagoshima University, 2.Nansei-Toku Observatory for Earthquakes and Volcanoes, Graduate School of Science and Engineering, Kagoshima University, 3.Institute of Seismology and Volcanology, Kyushu University

The earthquake (JMA Magnitude 7.1) occurred on November 14, 2015 in the area of west off Satsuma peninsula. The epicenter is located in Okinawa Trough where is in about 160 km west from Makurazaki City in Kagoshima Prefecture. This earthquake is one of the largest earthquakes in this area. Seismicity in this area is low in last twenty years. Two continuous GNSS sites are operated by Kagoshima University, one is UJIS site in Uji island which is 84 km to east from the epicenter and the other is MESM site in Meshima island which is 121 km north from the epicenter. At UJIS seismic observation is also operated by Kagoshima University and it is operated by Kyushu University at MESM. We went to those sites in order to get GNSS and seismic data because GNSS and seismic data are not telemetered at those sites. In this research, co-seismic crustal deformation and activity of aftershocks are reported. We relocated the main shock and aftershock until 10:00 on November 16. Length of aftershock area is about 60 km. Its Strike is the same of Okinawa Trough. The epicenter of the main shock is located at the south-west end of the aftershock area and maximum aftershock, which is occurred on November 15, is at north-east end. Activity of aftershock in northern part of aftershock area is high. However, in southern part it is low except aftermath of occurrence of the main shock. GNSS data analysis is by Bernese GNSS software Ver. 5.2 with CODE precise ephemeris. Daily site coordinates of UJIS and MESM are calculated with GEONET sites. Coseismic deformation is estimated by the difference between two days averages before and after the main shock. Displacement at UJIS and MESM is 0.82 cm and 0.65 cm, respectively. The theoretical coseismic deformation is estimated by a strike slip fault model (Okada, 1992). Fault length, strike, dip angle and fault position are estimated by the length of aftershock area. Fault width is assumed a half of the fault length. Amount of fault slip is estimated by the relationship between earthquake magnitude and moment (Sato, 1979). JMA moment magnitude 6.7 is used (JMA, 2015). Theoretical displacement at UJIS and MESM is 1.3 cm and 1.1 cm. Direction of observed displacement is coincident with that of theoretical displacement. However, amount of observed displacement is smaller than theoretical one.

Surface deformation associated with the Meinong, Taiwan, earthquake

*Manabu Hashimoto¹

1. Disaster Prevention Research Institute, Kyoto University

A Mw 6.4 earthquake hit southern Taiwan on February 6, and claimed more than 100 casualties due to the collapse of building. In order to detect surface deformation associated with this earthquake, we analyzed ALOS-2/PALSAR-2 images provided by the Japan Aerospace Exploration Agency (JAXA). Post-event observations were made on February 9 and 14 with strip-map mode from the ascending orbit and with ScanSAR mode from the descending orbit, respectively. ScanSAR mode image covers the entire southern half of Taiwan including the epicenter. Therefore we can discuss total image of earthquake. We performed 2-pass interferometry with Gamma software with ASTER-GDEM ver. 2. In ScanSAR interferogram, we found a 20 km x 20 km are of increase of line-of-sight (LOS) up 9 cm and a 10 km (EW) x 20 km (NS) zone of LOS decrease up to 12 cm. The latter zone is also recognized in the strip-map mode interferogram, implying that this zone uplifted. These results are consistent with the GNSS observations and interpretation that the thrust motion on a shallow dipping decollement is responsible for this event (Ching et al, 2016, personal communication).

It is interesting that there is a zone of LOS increase sandwiched by two LOS decrease areas. There is a report that cracks were found in the peripheral region of this LOS increase zone (Ray Chuang, personal communication). This observation implies that a subsidiary faulting may have occurred near the western edge of decollement.

We also found LOS increase in northeastern part of the Tainan city. This area is an alluvial plane near a river. Therefore we suspect that liquefaction occurred in this area.

We will visit Tainan and make a field reconnaissance. We will report the results of field reconnaissance as well.

ALOS-2/PALSAR-2 images were provided by JAXA through the activity of SAR analysis Working Group of the Coordinating Committee for Earthquake Prediction. The ownership and copyright of ALOS-2/PALSAR-2 images belong to JAXA.

Keywords: 2016 Meinong Taiwan earthquake, surface deformation, SAR, ALOS-2/PALSAR-2

Block Rotation and Intra-plate Deformation in Java, Indonesia based on GPS observations

*Henri Kuncoro¹, Satoshi Miura¹, Irwan Meilano², Susilo Susilo³

1.Graduate School of Science, Tohoku University, 2.Geodesy Research Division, Institute Technology of Bandung, 3.Geospatial Information Agency of Indonesia

Using the 1998-2013 horizontal velocity field including continuous and campaign Global Positioning System (GPS) phase data, we interpret the kinematics of Sunda Block and the present deformation of Indonesia. Four major earthquakes, the 2006 Java (M7.7, e.g. Ammon et al., 2006), The 2009 West Java (M7), and the 2012 Indian Ocean earthquakes (M8.6 and 8.2) occurred around southern boundary of the Sunda Block that affected the horizontal velocity field within the block. Since we only have the short span of time series for several sites especially in the Java island, we should remove the offsets and the exponential or logarithmic trends in the time series due to the earthquakes. By means of TDEFNODE (McCaffrey, 2009), we invert GPS site velocities simultaneously to estimate the Euler rotation parameter of blocks, earthquake slip vectors, and uniform horizontal strain rate tensor within the blocks. We constructed several block models for the Sunda Block kinematics and deformations. We assume one to four faults extending from the western part off the southern coast of Java and estimate the slip distributions. We also assume the different constraints on the nodes on these faults. From a series of the block models, we determine a preferred model by applying F-distribution tests between two models. The preferred model here is the one consisting of four faults along the Java trench with unconstrained nodes without a homogeneous strain rate tensor, and produces the reduced chi-square of 0.754. This model generates the Euler rotation parameters of 48.917°N for latitude, 86.876°W for longitude, and $0.330 \pm 0.002^\circ/\text{Myr}$ for angular velocity with an error elliptic axes of 0.96° and 0.15° for the pole location. The distributions of interseismic locking on the plate boundary along the Java trench demonstrates the low coupling rate of ~ 30 mm/yr in the western part, the very low rate < 10 mm/yr in the middle part, and the very high rate of ~ 65 mm/yr in the eastern part. The residual velocities derived from this model indicate the effect of the postseismic deformation in the western part of Java and the extensional pattern in the eastern part of Java, which may suggest volcanic deformation.

References:

Ammon, C. J.; Kanamori, H.; Lay, T.; Velasco, A. A. (2006), "The 17 July 2006 Java tsunami earthquake" (PDF), *Geophysical Research Letters* (American Geophysical Union) 33 (24): 1, doi:10.1029/2006gl028005

McCaffrey, R. (2009), "Time-dependent inversion of three-component continuous GPS for steady and transient sources in northern Cascadia", *Geophysical Research Letters*, 36, L07304, doi:10.1029/2008GL036784

Keywords: Sunda Block, Euler rotation, Block kinematics

Vertical displacement in Naruko Volcano area after the 2011 Tohoku earthquake deduced from precise leveling survey

*Naoko Takahashi¹, Masayuki Hatakeyama¹, Haruhi Yurimoto¹, Yuuki Honda¹, Yuya Tsukamoto², Akio Goto³, Yusaku Ohta⁴

1.Division of Earth and Planetary Materials Science, Faculty of Science, Tohoku University, 2.Department of Earth Science, Graduate School of Science, Tohoku University, 3.Center for Northeast Asian Studies, Tohoku University, 4.Research Center for Prediction of Earthquakes and Volcanic Eruptions, Graduate School of Science, Tohoku University

Great East Japan Earthquake occurred on 11 March 2011, causing large crustal deformation in the Tohoku region. GEONET observed subsidence exceeding 1m at Pacific coast and becoming smaller toward west (<http://www.gsi.go.jp/common/000059956.pdf>). To detect the vertical displacement inland, the first leveling survey was conducted in Naruko area, Miyagi prefecture, on east-west direction using a second-order leveling route along the National Route 47 for 10km in August 2011, as a part of summer field seminar by the Division of Earth and Planetary Material Science, Tohoku University. Contrary to the expectation before the survey, the subsidence increased westward in this section as compared with the leveling results in 2009 by Geospatial Information Authority of Japan (Tsukamoto et al, 2014). By In-SAR analysis, Ozawa and Fujita (2013) and Takada and Fukushima (2013) showed that Kurikoma-Naruko volcanic region subsided locally coincident with the earthquake. The westward relative subsidence detected by the leveling was in harmony with these results. The second leveling survey in August 2013 showed that further subsidence had progressed on the same route, and the displacement pattern was almost similar to that in 2011 (Tsukamoto et al, 2014).

To detect the subsequent displacement, we made the third precise leveling survey on 27-31 August 2015 on the same leveling route (benchmark number 047-064, 066, 068, 070, 072, 074 from east-west; hereafter indicated as BM64, BM66, etc.). We used bar-code leveling rods (Leica GPCL3) and an electronic digital level (Leica DNA03). We conducted round-trip survey between each benchmarks, and all residual errors fell within the acceptable range of the first-order leveling.

Relative to August 2013, BM66, BM68, BM72, and BM74 subsided 7.6 mm, 14.6 mm, 31.8 mm and 36.2 mm, respectively, against the eastern end BM64. These indicate westward-growing subsidence has continued (or probably is still continuing) along the survey route after August 2013, although the deformation rates have decelerated. The only exception is BM70; subsidence had changed into 4.6 mm uplift. This is the only uplift we have detected on this survey route since the 2011 Great Japan Earthquake.

Postseismic vertical displacements detected by GPS array, equipped semi-parallel to National Route 47 by Tohoku University, indicate that the surveyed area corresponds the transition zone from eastern uplift to western subsidence. Relative to the GPS station 0174 whose longitude is close to that of BM64, the next two western GPS stations collateral to the survey area have been subsiding, which is in harmony with our survey results. On the contrary the uplift such as seen at BM70 is undetected.

Leveling surveys in 1969 and 2009 by the Geographical Survey Institute indicate that BM70 subsided against BM68 while BM72 and 74 uplifted during this period. According to Prima and Yoshida (2010) and Ogawa et al. (2014), the eastern edge of the rim of Naruko caldera crosses between BM68 and BM70. The unique behavior of BM70 may be caused by such local geologic structure.

Keywords: Great East Japan Earthquake, Naruko caldera, precise leveling survey, subsidence

Precursory Strain and Tilt Variations of Earthquake Swarm Occurring in Izu Peninsula in March 1997 and Occurrence of M5.5 Earthquake.

*Hiroshi Ishii¹

1.Tono Research Institute of Earthquake Science, Association for the Development of Earthquake Prediction

Izu Peninsula is located at about 100km southwest of Tokyo. Earthquake swarms occurred in 1995, 1996, 1997 and 1998. We analyzed data observed by multi-component borehole instrument installed at swarm occurring area. The instrument equipped with strain meters, tilt meters, seismometers, magnetometers and a thermometer. Preliminary analyses were already reported. This time we investigated earthquake swarm occurring in 1997. Earthquake swarm started about 10:30 3/3 1997. Some results obtained are as follows:

1. Depth of hypocenters became shallower with about rate of 200m/hour after swarm occurred.
 2. Descending vectors of tilt indicate that after March 2nd vectors show abnormal variations and after the occurrence of swarms variation accelerated and M5.5 earthquake occurred.
 3. Principal strain variation recorded abnormal variations after the swarm occurred and variation accelerated and M5.5 earthquake occurred.
 4. Variations of tilt and strain become clarified from the beginning of occurrence to the end.
- We also discuss relationship between earthquakes and tilt/strain variations.

Keywords: Precursory Phenomena, Earthquake Swarm in Izu Peninsula, Multi-component Borehole Instrument for Crustal Activity Observation, Strain Variation, Tilt Variation

Permeability change due to the earthquake estimated by using atmospheric effect on groundwater migration

*Atsushi Mukai¹, Shigeaki Otsuka², Yoichi Fukuda³

1.Faculty of Urban Management, Fukuyama City University, 2.Faculty of Humanities and Sciences, Kobe Gakuin University, 3.Graduate School of Science, Kyoto University

Groundwater migration due to atmospheric loading variation is dependent on hydraulic property in aquifer. Therefore, observed atmospheric effects on groundwater discharge and pore pressure have some information about permeable structure in the surrounding crust. In this study, we estimated permeability and storage coefficient changes due to the 2011 off the Pacific coast of Tohoku Earthquake by using atmospheric effects on groundwater discharge and pore pressure observed in the fault fracture zone, and considered cause of their changes.

Groundwater migration due to atmospheric loading is considered to mainly occur in a fracture zone, because permeability in that area is higher than the surrounding crust. Mukai et al.(2015) made a one-dimensional groundwater migration model, in which groundwater is assumed to migrate laterally in fracture zone, and derived the theoretical equation showing frequency dependence of atmospheric effect on groundwater discharge. When this theoretical equation is applied to the observed atmospheric effect on groundwater discharge, we can estimate change of value ' $k \cdot S$ ' multiplying permeability ' k ' by storage coefficient ' S '.

We can also obtain the theoretical equation showing frequency dependence of atmospheric effect on pore pressure by using the above groundwater migration model. One of the variables for this theoretical equation is ' S/k ' dividing storage coefficient ' S ' by permeability ' k '. Thus, it is possible to estimate permeability and storage coefficient independently by analyzing both atmospheric effects on groundwater discharge and pore pressure.

We estimated change of permeability and storage coefficient in the fracture zone of Manpukuji fault, which is penetrated by the Rokko-Takao station, by using groundwater discharge and pore pressure observed at the station as well as atmospheric pressure on the ground at the Kobe local meteorological office in period from August 2010 to December 2011. In this estimation, we first divided the period into some sections with length of 512 data (21.3 days) and calculated frequency dependence of atmospheric effect for each section. Secondly we applied the theoretical equation on the one-dimensional groundwater migration model to the observed atmospheric effects, and estimated permeability and storage coefficient changes as the most adequate model parameters.

Estimated storage coefficient increased by 3 times just after the earthquake. Mukai and Otsuka (2012) estimated change of groundwater source pressure by using the model on groundwater migration from the source to the station. They reported that the groundwater source pressure decreased just after the earthquake and had not recovered for a few months. These results suggest that seismic motion induced outflow of mud accumulated in the cracks and excessive outflow of groundwater in the groundwater source and the surrounding crust.

Estimated permeability decreased by about 40% just after the earthquake. This result appears to disagree with the above conjecture that seismic motion induced the outflow of mud. This disagreement might be caused by inhomogeneous variation in permeability in the crust. It is considered that the permeability estimated in this study shows that near the station, because periodic atmospheric loading causes groundwater flow in a small scale. The mud outflow owing to seismic motion might have been concentrated near the station where groundwater discharge occurs, which in turn might have caused the decrease in permeability in that area.

Keywords: permeability change, groundwater migration, 2011 off the Pacific coast of Tohoku Earthquake

Real-time monitoring of crustal deformation

Takahiro Tsuyuki¹, Sin Chikazawa¹, Rie Tanada¹, *Hisao Kimura¹, Hiroshi Hasegawa¹, Akane Numano², Naoyuki Yamada¹, Masaki Nakamura¹, Tetsuo Hashimoto¹, Kazuki Miyaoka³

1.Japan Meteorological Agency, 2.Shizuoka Meteorological Office, 3.Meteorological Research Institute

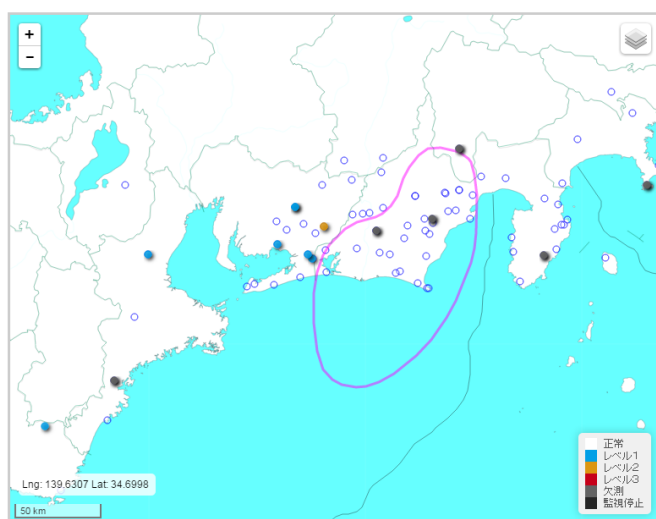
Japan Meteorological Agency is equipped with the new computer system to monitor crustal deformation, earthquake and tsunami. One of the purposes of this system is to detect precursor of the Tokai earthquake quickly and automatically. We introduce the stacking method (Miyaoka, Yokota, 2012) and the new idea which reduces 'ghosts', artificial changes of stacking data. The new system helps us to detect anomalous changes of plate boundary earlier.

Keywords: strainmeter, stacking, slow slip event

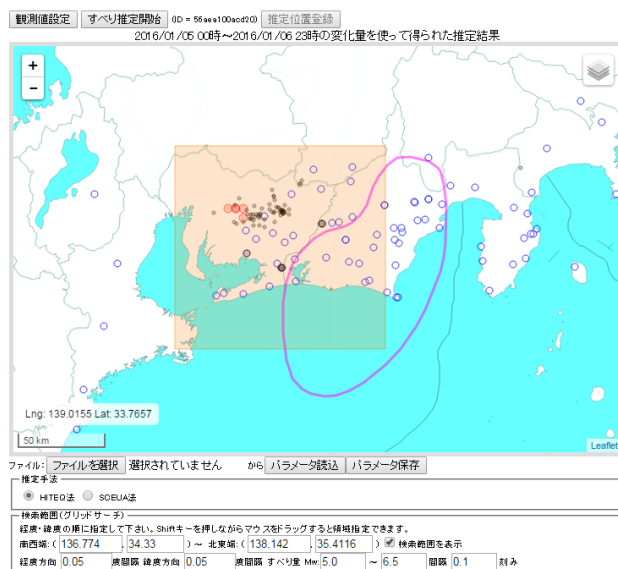
地殻活動総合監視画面

表示時刻: < 2016/1/5 8:35 > 最新 60分ごと 自動更新 更新停止 動画 印刷

2016/1/5 8:35 現在の状況



断層推定結果



Characteristic of inland strain anomalies caused by the postseismic deformation immediately after the 2011 Tohoku-Oki earthquake based on kinematic PPP data analysis

Yu'ichiro Hirata¹, *Yusaku Ohta¹, Mako Ohzono², Ryota Hino¹

1.Research Center for Prediction of Earthquakes and Volcanic Eruptions, Graduate School of Science, Tohoku University, 2.Department of Earth and Environmental Sciences, Faculty of Science, Yamagata University

We have investigated spatial and temporal development of anomalous crustal strain in the northeastern Japan region associate with a postseismic deformation immediately after the 2011 Tohoku-Oki earthquake. Ohzono et al. (EPS, 2012) found the characteristic strain anomalies associate with the step-like stress change caused by the large coseismic displacement. Their results, however, should contaminate the crustal deformation by the early postseismic within one day.

Based on these backgrounds, we adopted the kinematic precise point positioning (PPP) analysis for understanding the crustal deformation caused by the early postseismic immediately after the mainshock. We used GIPSY-OASIS II Ver. 6.3 software for kinematic PPP processing of whole GEONET sites in 10 March 2011. We applied every 6 hours nominal wet and dry zenith tropospheric delay value as a priori information based on the ECMWF global numerical climate model. For the coordinate time series and tropospheric parameters, we assumed white noise and random walk stochastic process, respectively. These unknown parameters are very sensitive to assumed process noise for each stochastic process. Thus, we searched for the optimum two variable parameters; wet zenith tropospheric parameter and its gradient.

Furthermore, we applied the principal component analysis for eliminate the spatial correlated noise from the kinematic PPP time series. The strain calculation from the displacement data is based on the method developed by Shen et al. (JGR, 1996). Obtained dilatation strain clearly shows the inhomogeneous distribution. Compared with the seismic tomography results by Nakajima et al. (JGR, 2001), large expansion area by this study mostly just correspond to the low Vp region at the 10km depth. This results suggested that these localized expansion areas correspond to the lower elastic moduli in the upper crust and/or shallower portion. Furthermore, we assessed the amount of strain anomalies by the early postseismic deformation relative to strain anomalies by the coseismic deformation. Our early postseismic results suggest that the 20-30% of strain anomalies by Ohzono et al. (2012) may be caused by the postseismic deformation. This result suggested that the early large postseismic deformation behaved as "step-like" stress change to the crust as well as the coseismic deformation.

Surface movements immediately before and after the 2011 Tohoku-oki earthquake from kinematic solution of GNSS and thermal expansion of the pillars

*Yuki Saegusa¹, Kosuke Heki¹

1.Department of Natural History Sciences, Graduate School of Science, Hokkaido University

The Tohoku-Oki earthquake (Mw9.0) occurred on March 11, 2011, and fault dislocation at the Japan Trench caused large eastward surface displacement of the Japanese Islands. Ohta et al. (2012) reported displacement of GNSS stations in NE Japan with the time resolution of three hours just before the Tohoku-Oki earthquake. Hino et al. (2014) reported high time-resolution vertical movements of the seafloor close to the epicenter using ocean bottom pressure gauge. Hirose (2011) analyzed the Hi-net tiltmeter data just before the Tohoku-oki earthquake. All these observations showed clear signatures of the afterslip of the foreshock that occurred two days before the main shock, but did not show any anomalous movement immediately before the earthquake.

For time periods just after the earthquake, Munekane (2012) reported kinematic analysis results of GNSS stations in NE Japan, and identified signatures of crustal deformation associated with several large foreshocks and the afterslip of the main shock fault. Mitsui & Heki (2012) analyzed periodic surface movements caused by the Earth's free oscillation. In addition to these "real" crustal movements, Munekane (2012) identified uniform horizontal displacement signatures, and inferred that they originate from differential thermal expansion of GNSS pillars due to direct sunlight.

In our study, we try to investigate spatial and temporal correlation between the sunshine and thermal-expansion origin horizontal displacements (see the attached figure). Here we used the 30-second position data of the GEONET station in NE Japan obtained using the RTnet software package by Dr. T. Iwabuchi, UNAVCO. This is the same data set that Mitsui and Heki (2012) used. We also use the weather data available from the website of Japan Meteorological Agency (<http://www.data.jma.go.jp/risk/obsdl/index.php>).

Description about the attached figure

[A]:Position change of the GNSS station (JST 12:00-13:00) by kinematic solution.

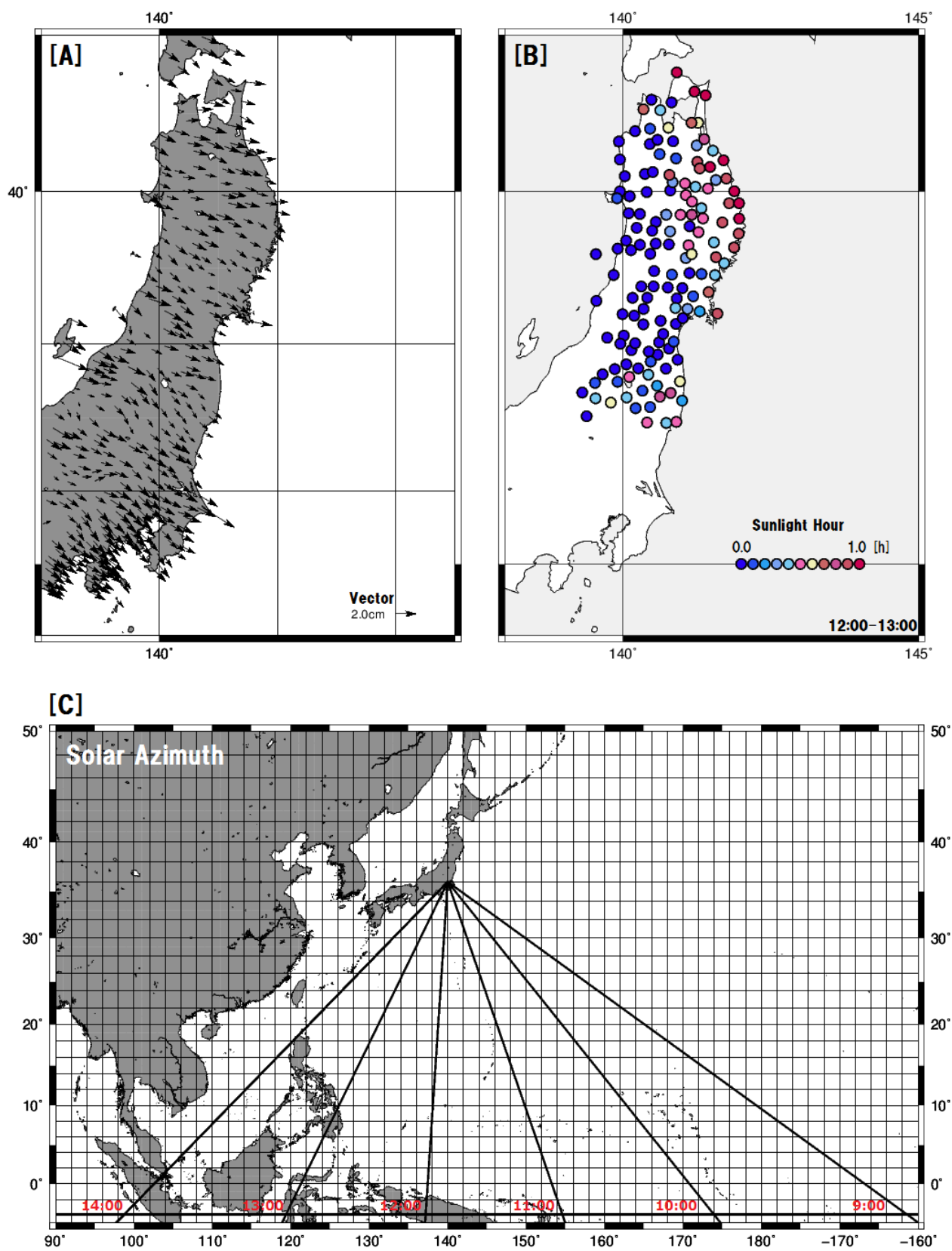
[B]:The sunlight hour (JST 12:00-13:00) by AMEDAS.

[C]:Solar Azimuth at every each hour.

Reference

- R. Hino, D. Inazu, Y. Ohta, Y. Ito, S. Suzuki, T. Iinuma, Y. Osada, M. Kido, H. Fujimoto, Y. Kaneda (2012):Was the 2011 Tohoku-Oki earthquake preceded by aseismic preslip? Examination of seafloor vertical deformation data near the epicenter, *Mar Geophys Res* (2014), 35, 181-190
- Y. Mitsui & K. Heki (2012):Observation of Earth's free oscillation by dense GPS array: After the 2011 Tohoku megathrust earthquake, *SCIENTIFIC REPORTS*, 2, 931
- H. Munekane (2012):Coseismic and early postseismic slips associated with the 2011 off the Pacific coast of Tohoku Earthquake sequence : EOF analysis of GPS kinematic time series, *Earth Planets Space*, 64, 1077-1091, 2012
- H. Hirose (2011):Tilt records prior to the 2011 off the Pacific coast of Tohoku Earthquake, *Earth Planets Space*, 63, 655-658, 2011
- Y. Ohta, R. Hino, D. Inazu, M. Ohzono, Y. Ito, M. Mishina, T. Iinuma, J. Nakajima, Y. Osada, K. Suzuki, H. Fujimoto, K. Tachibana, T. Demachi, S. Miura (2012):Geodetic constraints on afterslip characteristics following the March 9, 2011, Sanriku-oki earthquake, Japan, *Geophysical Research Letters*, Vol. 39, L16304

Keywords: crustal movement, GNSS, thermal expansion



Change of crustal deformations after the 2011 Tohoku-oki earthquake

*Hisashi Suito¹

1.GSI of Japan

Large displacements induced by the great earthquake occurred on March 11, 2011, were observed by GEONET over the entire Japanese Islands. The maximum horizontal displacement observed by the GEONET reaches 5.4m at the tip of the Oshika peninsula. The subsidence up to 1.1m was observed by the land GPS along the Pacific coast. The postseismic deformations caused by this great earthquake are still lasting over the northeast and central Japan area.

We report the change of postseismic deformations following the 2011 Tohoku-oki earthquake. We also report the mechanisms of these postseismic deformations.

Keywords: 2011 off the Pacific coast of Tohoku earthquake, postseismic deformation

Insight into poroelastic rebound deformation following the tohoku earthquake

*hidayat panuntun¹, SHINICHI MIYAZAKI¹

1. Graduate School of Science, Kyoto University

K. Wang, Hu, and He (2012) proposed 3 primary processes that dominate the deformation following an earthquake at subduction zones; (1) afterslip, (2) viscoelastic relaxation, (3) re-locking of subduction fault. However, if the upper crust was saturated by fluid, the crust must be treated as a fluid-saturated poroelastic medium instead of elastic medium. Coseismic stress change disrupts pore fluid equilibrium and causes fluid migration from high pressure to zone of low pressure. Fluid migration drives transient surface deformation which is known as poroelastic rebound. Pore fluid flow induced by coseismic stress change is usually ignored due to the fact that; (1) this effect occurs in short time at early postseismic deformation just around the rupture area, (2) and no clear evidence of fluid-rich existence in the upper crust of the rupture. Due to the fluid-rich existence detected in the upper crust (Z. Wang, Huang, Zhao, & Pei, 2012; Yamamoto, Obana, Kodaira, Hino, & Shinohara, 2014; Zhao, Huang, Umino, Hasegawa, & Kanamori, 2011), pore fluid flow induced by coseismic stress change can produce contribution to the surface deformation.

Therefore, poroelastic rebound should be included in the analysis of early postseismic deformation following the Tohoku earthquake. Previous modeling studies in poroelastic rebound used various values for undrained and drained Poisson's ratio (e.g., Peltzer, Rosen, Rogez, and Hudnut (1998); Jonsson, Segall, Pedersen, and Bjornsson (2003)). Instead of just assuming the values of drained and undrained Poisson's ratio, we use grid search to estimate undrained and drained Poisson's ratio value by combining forward calculation of poroelastic rebound and afterslip inversion of inland and offshore GPS data. In total, we build 400 poroelastic rebound models with different combinations of undrained and drained Poisson's ratio. Grid search approach obtained optimum values of 0.23 and 0.29 for drained and undrained Poisson's ratio, respectively. Poroelastic rebound produced by the optimum values of drained and undrained Poisson's ratio estimated horizontal displacement up to 0.28 m in the rupture area. Majority of large uplift due to poroelastic rebound occurred in and around the vicinity of the rupture area where maximum uplift estimated up to 0.37 m around the maximum slip area of the mainshock.

Keywords: poroelastic rebound, undrained and drained Poisson's ratio, grid search, co- and after-slip inversion

The slow slip event in the Tokai region, central Japan, since 2013 as seen from GPS data

*Hiromu Sakaue¹, Jun'ichi Fukuda¹, Teruyuki Kato¹

1. Earthquake Research Institute, The University of Tokyo

Advent and developments of continuously operating dense GPS arrays have enabled us to detect aseismic transient slow slips called as slow slip events (SSE) that occur along the subducting plate interface. SSE has been discovered in Bungo Channel, Boso Peninsula, Tokai region and Ryukyu region in Japan. Moreover, short term SSEs have been found using the data of tiltmeters in the Hi-net seismic network in the southwestern Japan. These short-term SSEs are often accompanied by non-volcanic or deep low-frequency tremors.

In the Tokai region, the previous long-term SSE occurred from 2000 to 2005, the longest SSE ever found. Ozawa and Yarai (2014) suggested the possible next SSE started to occur near the previous occurrence location in the beginning of 2013. Therefore, in this study, we analyzed the GPS data in the Tokai region to estimate the temporal evolution of the current event. The data for the period from 1 January 2008 and 30 April 2015 was used. The GIPSY-OASIS II software was used for estimating daily coordinates of the 226 GPS stations from the GEONET in the Tokai district. Then, the coordinate time series were fitted with linear trend and seasonal variations for the period before the 11 March 2011 Tohoku-oki earthquake (Mw9.0). The obtained linear trend was extrapolated to the end of data, 30 April 2015, and was subtracted from the original coordinate time series.

Then, the effects of the post-seismic deformation due to the Tohoku-oki earthquake were removed by fitting the data from 11 March 2011 to the end of the data with simple mathematical functions, not considering physical processes of the post-seismic crustal deformations. We employed a logarithmic function and a logarithmic plus exponential function to model the post-seismic deformation and found that the latter fits the data significantly better. We thus used the logarithmic plus exponential function to model and remove the post-seismic deformation.

After removing the post-seismic effects by the above pre-processing, we applied the time-dependent inversion method to the data to obtain the spatio-temporal evolution of slip beneath the Tokai region. For this purpose, we used a modified Network Inversion Filter (NIF) (Fukuda et al., 2008), which is a modification of the original NIF (Segall and Matthews, 1997). The original NIF assumes a constant hyperparameter for the temporal smoothing of slip rate and thus results in oversmoothing of slip rate. The modified NIF assumes a time variable hyperparameter, so that changes in slip rate are effectively extracted from GPS time series.

The results suggest that six short term SSEs were embedded in the slow and steady long-term SSE during the time interval from the beginning of 2013 to the end of April 2015. We investigated the detected short term SSEs in more detail. The results shows: first, rapid SSEs occurred from October to December 2013 and from August to October 2014 which were accompanied by low frequency tremors. Then, a rapid SSE occurred from the beginning of January to February 2014 around the Ise Bay. This SSE was also accompanied by low frequency tremors. Finally, another SSE was found in April 2015 and this SSE was also accompanied by low frequency tremors.

The results indicate that the maximum slip for the long term SSE from 1 January 2013 to 30 April 2015, was estimated to be about 6 cm and the large slip was located in nearly the same area as or slightly to the south of the previous event. This long term SSE is still continuing at the end of April 2015.

Crustal contraction of the Sado Ridge estimated from geologic structure, eastern margin of Japan Sea

*Yukinobu Okamura¹

1.Research Institute of Earthquake and Volcano Geology, National Institute of Advanced Industrial Science and Technology

The amount of crustal shortening in the Sado Ridge, eastern margin of Japan Sea, was estimated from geologic structure. Many reverse faults have developed in the Sado Ridge under the W-E compressional stress during the last 3.5 million years. The faults were Miocene normal faults that have reactivated by inversion tectonics. The about 70 km wide ridge extends to NNE for about 250 km from the Sado Island and consists of many reverse faults accompanying asymmetric anticlines of 10 to 20 km wide. Assuming that these anticlines are fault-related folds above reverse faults that cut entire upper crust, it is possible to estimate amount of crustal shortening from the area of anticline on seismic profile that is product of thickness of the upper crust and horizontal slip of the fault.

This study based on seismic profiles acquired by the Geological Survey of Japan from 1989 to 1991. They are single-channel data, but they have enough quality to identify geologic structure of several hundreds meters below seafloor. The direction of seismic survey lines is 290° sub-parallel to the direction of contraction of the eastern margin of Japan Sea, and interval of the lines is about 3 km.

The onset of the reverse faulting is widely recognized by an unconformity marked by the change of reflection pattern from parallel to divergent below and above of the unconformity, which indicate that the ridge was nearly flat before the reverse faulting and uplift of anticline changed depositional patterns. I determined the geometry of anticline from the unconformity horizon on the seismic profiles and the area of anticline was measured assuming the unconformity was flat before folding. Some anticlines were truncated at their summits and a few may be composed of basement which has no internal structure. I determined fold geometry of anticlines from structure of underlying and surrounding sediments. Fifty seismic lines were analyzed to estimate crustal shortening.

The Sado Ridge is composed of several sub-parallel chains of anticlines. Although the area of anticline varies along the chain, the sum of the areas of anticlines along the WNW trending seismic lines crossing the entire Sado Ridge shows smaller variation. The crustal shortening of the ridge was roughly estimated to be 2 km or less assuming that the thickness of the upper crust is 15 km. This analysis suggests that the direction of crustal shortening is more westerly directed than 290°. I also discuss the problems and significance of estimation of crustal shortening using geological structure.

Keywords: eastern margin of Japan Sea, crustal contraction, fault-related fold

Relation of decay time constants between postseismic deformation and aftershocks of the 2011 Tohoku-Oki earthquake

*Mikio Tobita¹

1.Geospatial Information Authority of Japan

Since the 2011 off the Pacific coast of Tohoku Earthquake (Tohoku-Oki earthquake), crustal deformation and aftershocks have continued to occur in eastern Japan. This paper discusses the comparison of their relaxation time constants.

1. Introduction

Tobita(2014, 2015, 2016) proposed combined logarithmic (log) and exponential (exp) function model for fitting postseismic GNSS time series after 2011 Tohoku-Oki earthquake. They are log+exp (Model-1), log+log+exp (Model-2) and log+exp+exp (Model-3). The Model-2 has the best performance for the short-term prediction of the evolution of postseismic deformation. The equation that represents the Model-2 is

$$D(t) = a \ln(1+t/b) + c + d \ln(1+t/e) - f \exp(-t/g) + Vt,$$

where $D(t)$ denotes a displacement component (east, north, or up), t is the time in days relative to the occurrence of the main shock (11 March 2011), b , e and g denote the timescale parameters of the logarithmic or exponential decays (relaxation times), and V is the steady velocity.

We believe that comparison of relaxation time parameters between cumulative number of aftershocks and the postseismic deformation may contribute to discriminate the subsurface postseismic deformation mechanisms.

As the first step, we began to study function fitting of aftershocks by Omori's formula, Modified Omori's formula and ETAS model, then attempt to adopt single exp and single log functions.

2. Methods and Results

The bold curve in Fig. 1 represents the cumulative number of aftershocks larger than M5 in the rectangle shown in the map in Fig. 1.

- (1) A single exponential function cannot fit the curve at all.
- (2) Fitting performance by a single logarithmic function is not satisfactory.
- (3) We found that a logarithmic function with background seismicity fits the cumulative aftershocks curve very well.
- (4) The first log term in the equation with relaxation time constants $b=0.03$ days (preliminary estimate) with the background seismicity (μ in Fig. 1) was fitted to the curve of the cumulative number of aftershocks.
- (5) The second log term in the equation with relaxation time constants $e=49.6$ days (preliminary estimate) with the background seismicity was fitted to the curve.
- (6) The third exp term in the equation with relaxation time constants $g=4610$ days (preliminary estimate) with the background seismicity was fitted to the curve.

The results of the three fittings (4)-(6) are shown in Fig. 1. While, the second term (log) with mid-term relaxation time (5) and the third term (exp) with long-term relaxation time (6) do not fit the curve at all, the first term (log) with short-term relaxation time (4) fit the curve quite well.

3. Discussion

We found that the relaxation time constants of the cumulative number of aftershocks are very similar to that of the first term (log) with short-term relaxation time of postseismic deformation time-series. Tobita (2016) suggests that the short-term log function may represent postseismic displacements due to mainly the afterslip, while the mid-term log and long-term exp functions may

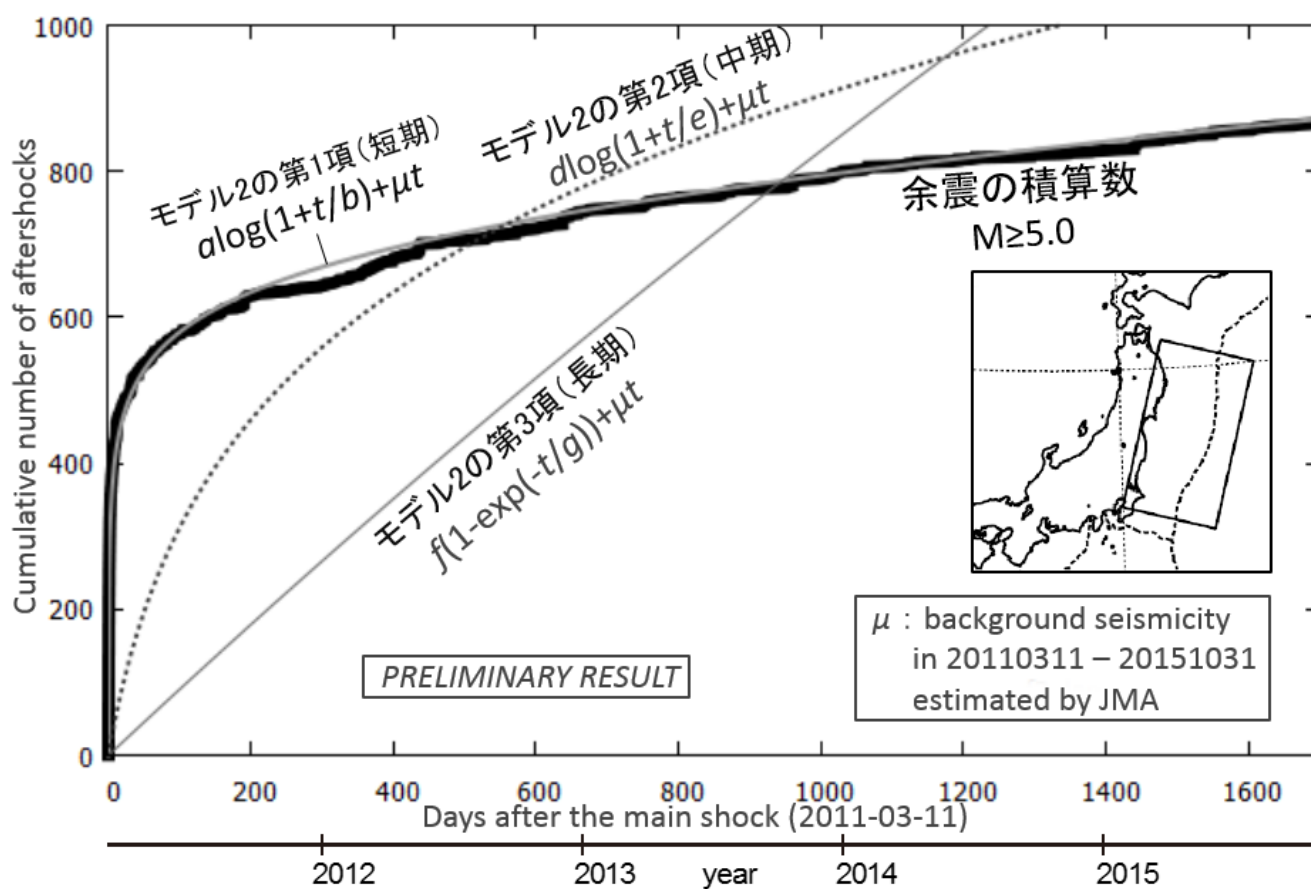
represent postseismic displacements due to mainly the viscoelastic relaxation. Our finding is consistent with the suggestion.

Good fits of the cumulative aftershocks curve by a single log function (with background seismicity) means validity of the Omori's law in the Tohoku-Oki earthquake, because the time integral of the Omori's formula is a logarithmic function.

Acknowledgement

The rectangle in Tohoku area, seismic data, and model parameters of the seismic data were provided by JMA. We appreciate it.

Keywords: 2011 Tohoku-Oki earthquake, postseismic deformation, function fitting, aftershock, viscoelastic relaxation, decay time



Time series modeling of the postseismic deformation after the 2011 Tohoku earthquake

*Shunsuke Miura¹, Mako Ohzono²

1. Department of Earth and Environmental Sciences Graduate School, Yamagata University, 2. Faculty of Science, Yamagata University

Time series of the postseismic deformation is often explained by superposition of the logarithmic and exponential time evolutions, which assumes the afterslip and the viscoelastic relaxation, respectively. For the 2011 Tohoku-oki earthquake (M9.0), eastern side of GNSS network is well explained by superposition of those functions (e.g., Tobita, 2015). Miura and Ohzono (2015) also explained postseismic time evolution using F3 daily solution at the 93 GEONET sites in wide region of Tohoku for four years after the earthquake. The estimated time constants of the horizontal component of afterslip and viscoelastic relaxation are ~7 days and ~2500 days, respectively. The vertical displacement has large signal of viscoelastic relaxation along the east coast of the study area. Focusing on spatial distribution of the estimated each signal for four years, we compare our result with other postseismic models. Our result of afterslip estimation shows large horizontal displacement of 100cm at Yamada in eastern part of Iwate. Around this site, from Kwai2 to Rifu in fore-arc relatively large displacements (< 80 cm). This pattern roughly agrees with other result of afterslip modeling (e.g., Silverii *et al.*, 2014; Yamagiwa *et al.*, 2014). On the other hand, some sites that have clear signal are not explained by the previous studies. The vertical displacement pattern, which shows obvious trend in the time series, may be cannot explained by the model. Although the maximum signal of the viscoelastic relaxation is smaller than that of the afterslip, it distributes more extensive region including back-arc side. This uniform displacement pattern will be mostly explained by simple viscoelastic model.

Keywords: postseismic deformation, tohoku earthquake

Heterogeneous surface deformation of the Kanto plain after the 2011 Tohoku earthquake

*Kazuya Ishitsuka¹, Takuya Nishimura², Toshifumi Matsuoka^{3,1}

1.Fukada Geological Institution, 2.Disaster Prevention Research Institute, Kyoto University,
3.Center for the Promotion of Interdisciplinary Education and Research, Kyoto University

Surface deformation of Japan island after the 2011 Tohoku earthquake has been modeled by visco-elastic relaxation and after slip. On the other hand, there were local post-seismic deformation at the Kanto plain that cannot be explained by the common model. In this study, we investigated surface deformation of the Kanto plain from March 2011 to December 2013 using GEONET data and PS-InSAR analysis of TerraSAR-X data. It has been reported that the Kanto region has uplifted after the 2011 earthquake, and the uplift velocity has been faster along with the distance from the epicenter. In addition to the global uplift pattern, we found the uplift velocity was locally faster about several mm/year around the north of Kanagawa Prefecture and the west of Tokyo. The local uplift occurred soon after the earthquake and decayed over about two years. As far as we know, sudden artificial changes such as groundwater usage were not reported in the period, accordingly this local uplift has likely occurred spontaneously. Moreover, our PS-InSAR analysis estimated the uplift occurred with the spatial dimension of about 10-20 km². This study of local post-seismic deformation may reveal local stress perturbation and a post-seismic deformation mechanism that has not been previously concerned.

Keywords: The 2011 Tohoku earthquake, The Kanto plain, Crustal deformation, GEONET, PS-InSAR analysis

Aseismic slips synchronized with earthquakes in northern Chiba Prefecture, Japan

*Akio Kobayashi¹, Fuyuki Hirose¹

1.Meteorological Research Institute, Japan Meteorological Agency

Episodes of intermittent uplift over periods of one month to a year have been observed by the Global Navigation Satellite System in the northeastern part of Chiba Prefecture, Kanto district, Japan. Uplift in the vicinity of Choshi in 2000 was accompanied by the earthquake near Choshi in June 2000 (M6.1). Uplift of the northeastern part of Chiba Prefecture in 2005 was accompanied by the earthquakes near Choshi in April 2005 (M6.1) and near Chiba-city in July 2005 (M6.0). Although our estimates of the source parameters for these uplifts were well explained by slips on the faults of these earthquakes, the amounts of slip we estimated for the uplifts were several times larger than we expected from the earthquakes. We attribute the extra slip to the above mentioned intermittent uplift events, which we suggest were caused by aseismic slips.

Keywords: Aseismic slip, Northern Chiba Prefecture, GNSS

Time dependent block fault modeling of southeast Japan

*Shinzaburo Ozawa¹

1.GSI of Japan

Abstract

We conducted time dependent block fault modeling for southeast Japan. The result shows that slip deficit on the Philippine sea plate which takes block motion into account becomes smaller than that which does not take into account block motion. In particular, slip deficit of the Philippine Sea plate in the Tokai inland area disappears, as was confirmed in previous studies by many researchers.

Introduction

It is very important to estimate interplate coupling precisely so that we can get information about whereabout and moment magnitude of the expected large subduction earthquakes. In particular, it is an urgent task to prepare for the Tokai and Tonakai earthquakes along the Suruga and Nankai troughs. Under this circumstance, many studies have been conducted about the interplate coupling in southeast Japan. However, spatial and temporal interplate coupling has not been treated in detail. In this study, we developed an analytical code of time dependent block fault modeling and applied it to southeast Japan.

Analytical Procedure

Hashimoto et al(2000) conducted block fault modeling of Japan, using GPS data. In this study, we used the block model geometry of Hashimoto et al. (2000). That is we used rectangular faults in inland area defined by Hashimoto et al. (2000). The plate boundary in a subduction area was represented by superposition of spline functions. By using this geometry, we estimated interplate coupling in inland area and subduction zones. We used EW, NS, UD position time series at approximately 500 GPS sites. The period was set at 2008-2009

Results and Discussion

Time dependent block fault modeling shows that interplate coupling on the Philippine Sea plate decreases when we take into account a block motion. In Tokai region, coupling on the Philippine Sea plate disappears in deep inland area.

Keywords: time dependent inversion, block fault modeling , southeast Japan

Abnormal strain distribution in Hokkaido, Japan, inferred from the 2003 Tokachi-oki earthquake (M8.0)

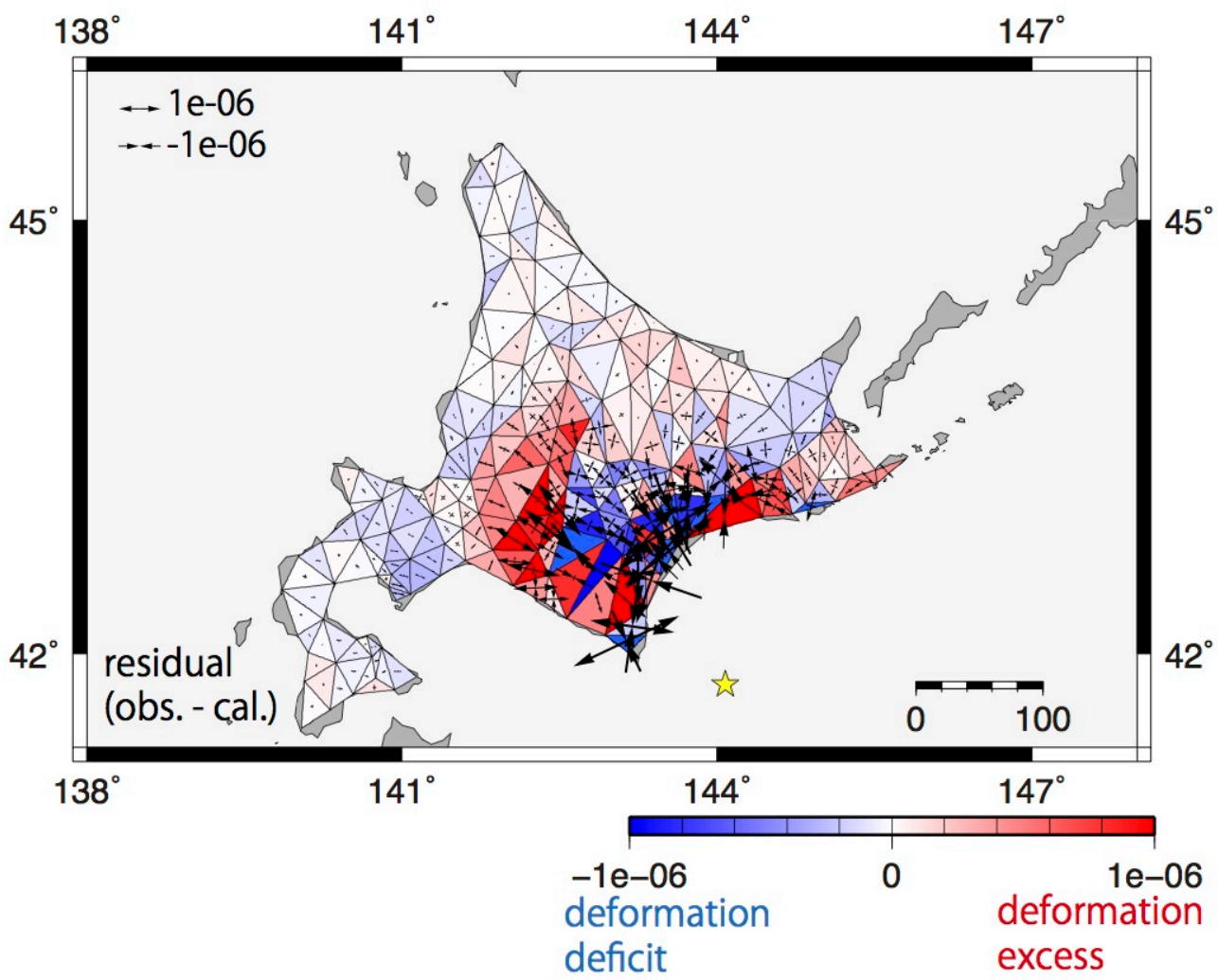
*Kentaro Ishimori¹, Mako Ohzono²

1.Department of Earth and Environmental Sciences Graduate School, Yamagata University, 2.Faculty of Science, Yamagata University

From the coseismic strain distribution of the 2003 Tokachi-oki earthquake (M8.0) and 2011 Tohoku-oki earthquake (M9.0), we try to examine how big abnormal coseismic strain can correlate to heterogeneous subsurface structure in Hokkaido, Japan. For the 2003 Tokachi-oki earthquake, Ishimori and Ohzono (2015, JpGU) compared coseismic crustal deformation observed from GEONET F3 solutions with theoretical crustal deformation which calculated from dislocation model (Okada, 1992) with a rectangular fault. The result shows 10^{-7} of strain anomaly (difference between observations and calculations), and good agreement of spatial distribution of the strain anomaly region and characteristic subsurface structure, such as thick sedimentary area. This feature is supported by a simulation that suggests the relatively small elastic moduli of the thick sedimentary layer in the upper crust (Yabe et al., 2015). We also estimate the coseismic strain anomaly in Hokkaido at the 2011 Tohoku-oki earthquake. As a result, we found 10^{-8} of coseismic strain anomaly. However, the relationship between the strain anomaly distribution and subsurface structure was not clear. We conclude that that the tiny strain anomaly ($<10^{-7}$) cannot detect characteristic subsurface structure.

For the coseismic strain anomaly of the 2003 Tokachi-oki earthquake, the vectors of principal maximum strain calculated from residual displacements (observations - calculations) indicates relatively large NW-SE convergence axes in eastern part of Hokkaido (Kushiro-Nemuro region). On the other hand, middle size of interplate earthquake, such as 2004 Kushiro-oki earthquake (M7.1) is occurred after the Tokachi-oki earthquake (2003, 1952). Because residual convergence direction agrees with the plate convergence direction, there is a possibility that those earthquakes might be triggered by the large coseismic strain anomaly.

Keywords: 2003 Tokachi-oki earthquake, subsurface structure, abnormal strain



Coseismic and Postseismic Deformation Related to The 2012 Indian Ocean Earthquake using Three-Dimensional FEM

*Cecep Pratama¹, Takeo Ito^{1,2}, Fumiaki Kimata³, Takao Tabei⁴

1.Graduate School of Environmental Studies, Nagoya University, 2.Earthquake and Volcano Research Center, 3.Tono Research Institute of Earthquake Science, 4.Department of Applied Science, Faculty of Science, Kochi University

On April 11, 2012, a Mw 8.6 earthquake struck off the west coast of northern Sumatra approximately 100 km west of the Sunda trench. The 2012 Indian Ocean earthquake, which is the largest intraplate earthquake in recorded history, yields a total seismic moment of 13.6×10^{28} dyne cm. Aceh GPS Network for Sumatran Fault System (AGNeSS) observed a predominantly ENE coseismic offset of up to 10 cm while the sites on the Andaman Island and southern part of Sumatra GPS Array (SuGaR) network observed southward and northward, respectively. In order to construct more realistic surface displacement due to complex subduction region, we consider developing inhomogeneous three-dimensional finite element model incorporate subducting slab, three-dimensional velocity earth structure, realistic topography and bathymetry. We infer uniform slip for six fault planes using fault geometry as reported from Hill et al. (2015). In the other hand, the time series of continuous GPS site coordinates clearly exhibit postseismic displacements. We parameterized the displacements time series due to previous earthquakes and remove pre-earthquake trend from the time series. The corrected time series of permanent GPS data shows that the relaxation time in the vertical component displacement is longer than horizontal component displacements. This discrepancy indicates multiple physical mechanisms. We proposed a mechanical model, which refer to afterslip and viscoelastic relaxation, to explain postseismic deformation following to the 2012 Indian Ocean Earthquake.

Keywords: Coseismic, Postseismic, GPS, FEM

Investigating the crustal deformation on the Hazar-Palu segment of the East Anatolian Fault (EAF), Turkey

*WUMITI JULAITI¹, Semih Ergintav¹, Ziyadin Cakir², Ugur Dogan³, Selver Senturk², Seda Cetin³, Hayrullah Karabulut¹, Fuat Saroglu, Haluk Ozener¹

1.Bogazici University, 2.Istanbul Technical University, 3.Yildiz Technical University

As well known, strike-slip faults are a fault type widely spread around the world. Many of them are located at boundaries between two tectonic plates. For instance, the East Anatolian Fault (EAF), the one in this study, forms a 400-km-long boundary between the Anatolian and the Arabian plates. It is a typical left-lateral slip fault with an ENE-WSW strike and a total offset of 33 km. As it is easy to obtain velocity solution from GPS raw data on a specific block or plate with the software, here is GAMIT/GLOBK, one can estimate the long-term slip rate as well as creeping zone, locking depth and the offset between two nearly-rigid blocks of a fault or between the fault's surface trace and the dislocation below the seismogenic zone by using inter-seismic GPS velocities and proper models. However, not many suchlike studies have been carried out along the whole EAF as those done on North Anatolian Fault (NAF) during the last 20 years. Most of them are focused on the area around the triple junction where the Dead Sea Fault connects to the EAF and the overall deformation using mainly InSAR. Moreover, there are only a few large earthquakes documented since the last century and InSAR based studies indicate that low seismicity can be related with a creep mechanism that may reach to 10 mm/yr creep rate, along different segments of the EAF. Based on the recent published GPS velocities, the slip rate on EAF is estimated about 8 to 10 mm/yr, which seems that the strain accumulation will not occur and therefore the creeping zone of EAF will not produce a remarkable earthquake. But the extent of the creeping zone is not well constrained, which still implies the potential of the seismic hazard arising.

The aim of this study here is to perform the velocity solutions from the present-day cGPS sites' data (Turkey's National Permanent GPS Network-ACTIVE data, i.e. TUSAGA-ACTIVE data) and new sGPS observations (up-to-date surveys based on proper profiles) on particular segment of EAF, the Hazar-Palu segment, which may be combined with the more recent InSAR observations, to develop an appropriate inter-seismic deformation model around this region with a multidisciplinary perspective.

Keywords: creep, GPS, East Anatolian Fault, slip rate

Computation of uplift rate caused by present-day ice melting in Southeast Alaska

*Kazuhiro Naganawa¹, Takahito Kazama¹, Yoichi Fukuda¹

1. Graduate School of Science, Kyoto University

Crustal uplift caused by ice melting is observed in glacial areas such as Antarctica, Greenland and Alaska. This uplift consists of elastic and viscoelastic effects, which are called post glacial rebound (PGR) and present-day ice melting (PDIM), respectively. By dividing these effects from observed geodetic data, geophysical parameters such as mantle viscosity can be estimated.

In Southeast Alaska, for example, many geodesists have studied spatiotemporal characteristics of the crustal uplift due to ice melting. Sun et al. (2010) collected absolute gravity values in Southeast Alaska once a year from 2006 to 2008, and calculated the rate of the uplift due to PDIM ($d\Delta/dt$) from the absolute gravity and GPS data. They also estimated the $d\Delta/dt$ values by the spatial integral of a PDIM model, showing the spatial distribution of the ice melting rate around Southeast Alaska. However, the amplitudes of the $d\Delta/dt$ values were not consistent with each other, possibly because Sun et al. (2010) simplified the conditions of their model calculation, especially about the distance between glaciers and each gravity site.

We were thus motivated to accurately estimate the rate of the PDIM-derived uplift at six absolute gravity sites in Southeast Alaska using PDIM models and observed geodetic data ($d\Delta/dt(\text{obs})$ and $d\Delta/dt(\text{cal})$, respectively). We first calculated $d\Delta/dt(\text{cal})$ by the spatial integral of the UAF07 PDIM model (Larsen et al., 2007) using a response function of crustal deformation to a disk load (Farrell, 1972). We also calculated $d\Delta/dt(\text{obs})$ from the rates of the GPS uplift and absolute gravity change from 2006 to 2013 (Kazama et al., 2015) using equations based on Wahr et al. (1995).

The average value of $d\Delta/dt(\text{obs})$ at six gravity sites was calculated to be 14.7 ± 2.2 mm/year, and its standard deviation is smaller than that of Sun et al. (2010) (10.7 ± 7.3 mm/year) because we utilized the precise values of the gravity variation rates by Kazama et al. (2015), who considered the absolute gravity data newly obtained in 2012 and 2013. In addition, the average value of $d\Delta/dt(\text{cal})$ was estimated to be 10.3 ± 1.4 mm/year, which corresponded to 70 % of $d\Delta/dt(\text{obs})$ in this study. Our $d\Delta/dt(\text{cal})$ value reproduced the $d\Delta/dt(\text{obs})$ value more than that of Sun et al. (2010) (5.5 ± 3.2 mm/year; 50 % of their $d\Delta/dt(\text{obs})$ value), because we considered realistic distributions of glaciers and gravity sites in estimating $d\Delta/dt(\text{cal})$ from the PDIM model. The $d\Delta/dt(\text{cal})$ value in this study still differs with $d\Delta/dt(\text{obs})$ by about 30 %, which implies that more realistic conditions should be considered in the model calculation, such as the curvature, topography or internal structure of the Earth, and/or updated PDIM models.

Keywords: load deformation, ice sheet melting, gravity change, crustal uplift, Alaska

Spatial variation in Earth structure inferred by GNSS seasonal deformations due to snow loads

Rie Kurisu², *Hitoshi Hirose¹, Takuya Nishimura³

1.Research Center for Urban Safety and Security, Kobe University, 2.Graduate School of Science, Kobe University, 3.Disaster Prevention Research Institute, Kyoto University

Seasonal variations are observed in GNSS site coordinate time series (e.g., Murakami and Miyazaki, 2001; Munekane et al., 2004). Heki (2001) showed that snow loads cause seasonal subsidence in winter in the Tohoku region, northeast Japan from the Geospatial Information Authority of Japan's (GSI) GEONET GNSS daily site coordinates during the period 1999.0-2001.0. It becomes worth reevaluating this issue because the observed GNSS data are accumulated over 10 years and the amplitude of apparent seasonal components can be reduced with revised analysis strategies (e.g., Nakagawa et al., 2009). Here we show that the correlation between a seasonal variation and snow depth over 10 years is good in some areas with the largest snow depths among the study areas, the ratio of seasonal subsidence to snow depth shows spatial variation, and the variation can be explained by spatial variation of underground structure.

We obtain daily coordinate time series at GEONET sites in the Tohoku region by applying GIPSY-OASIS II software (version 6.3) (Zumberge et al., 1997) to observed phase data provided by GSI. A seasonal signal in vertical component for each year is estimated for each site. These seasonal signals are compared with daily snow depth measurements at AMeDAS sites. We use data at 135 GEONET sites and 102 AMeDAS sites in the Tohoku region during the period 1999.5-2009.5.

The Tohoku region is divided into a number of areas as large as 0.5 degree in latitude and 0.5 degree in longitude in order to find spatial variation in the correlation between the seasonal signal and the snow depth. We calculate an averaged seasonal signal for each area from the seasonal signals of individual GEONET sites in the area. Similarly, an averaged snow depths are calculated for each area. These averages are converted to time series of monthly values. We find a correlation coefficient larger than 0.6 on most areas with the maximum averaged snow depth > 150 cm. We estimate the ratio of seasonal subsidence to snow depth (defined as "the ratio b") from the monthly values on these areas. The ratio b of the range 0.021-0.053 mm/cm is obtained from five areas among eight areas where maximum snow depths are higher than 150 cm (three areas are eliminated because subsidence due to pumping of groundwater in winter is suggested).

For comparison with the observed ratio b, we compute the expected ratio b assuming the Gutenberg-Bullen A Earth model (Sato et al., 1968) with snow density of the range 0.2-0.5 g/cm³ (Kawashima et al., 2007) using SPOTL (Agnew, 1996). In this case, the ratio b of the range 0.0083-0.021 mm/cm (defined as "b_{basement}") is expected. b_{basement} is smaller than the observed ratio b, indicating that the observed subsidence is larger than the calculated one assuming a global Earth model without a softer sediment layer.

Next we estimate the ratio b for a sedimentary basin because the study area includes Niigata basin where one of the thickest sediment layer is observed in Japan. Assuming averaged values of V_p, V_s, and for the Niigata sediment layer (Koketsu, 2008), Young's modulus of 7.2 GPa, and then the strain of 2.7-6.8e-7 are obtained under the same snow load as b_{basement}. Assuming that deformation caused by snow load occurs in the sedimentary layer with the thickness of 8 km (J-SHIS, <http://www.j-shis.bosai.go.jp>), subsidence of 2.2-5.4 mm and the ratio b (b_{sediment}) of 0.022-0.054 mm/cm is expected. Although this estimation is very rough, the ratio b_{sediment} can explain the observed ratio b, which is larger than b_{basement}. Therefore, the spatial variation of the ratio b observed by GNSS can not be explained by the variation in snow density only, and an

additional amplifying factor, possibly an effect of softer sedimentary layer, must be required. This study shows a possibility to be able to probe the spatial variation of the elastic response to snow loads with GNSS.

Keywords: Deformation by surface load, Seasonal variation in crustal deformation, Sedimentary layer

Theoretical calculation of internal stress/strain changes caused by earthquakes: the effectiveness of the reciprocity theorem in a spherical earth

*Yu Takagi¹, Shuhei Okubo²

1.School of Science, The University of Tokyo, 2.Earthquake Research Institute, The University of Tokyo

Co-seismic deformation (e.g. stress and strain changes) within the Earth has been estimated by using Okada's (1992) formulae for a semi-infinite homogeneous medium. An example is seen in estimation of Coulomb's static stress changes. However, when stress or strain changes caused by great earthquakes are estimated, we should use a more realistic earth model including the effects of Earth's curvature and layered structure; the stress changes caused by the 2011 Tohoku-oki earthquake exceed 0.1 bar even at the epicentral distance over 400 km (Toda et al., 2011). In principle, Takeuchi & Saito (1972) showed a recipe to calculate deformations due to earthquakes in a spherical earth model. In practice, however, there are some computational problems in order to realize the computation of internal deformations. One of them is loss of significant digits (LSD). We found that a method using the reciprocity theorem (Okubo, 1993) can avoid this problem. In this presentation, we will show that the conventional method cannot avoid the LSD whereas the method using reciprocity theorem can.

After Takeuchi & Saito (1972), the equations governing co-seismic deformation field result in first-order inhomogeneous differential equations by expanding displacement and stress by the spherical harmonics. To solve these differential equations, in the conventional method, (i) we obtain the complementary solutions, (ii) find the particular solution, and (iii) add them so that the final solution satisfies the surface boundary condition. The magnitude of the final solution is the order of $(r_s/r_p)^n$, where the r_s and r_p ($>r_s$) are the radii where the source is located and the deformation is evaluated, respectively, and n is the degree of the spherical harmonics. On the other hand, the magnitude of the solutions obtained by the process (i) and (ii) is the order of $(r_p/r_s)^n$. This means that, in process (iii), LSD cannot be avoided at a large degree n because we need to add the numbers whose magnitude is $(r_p/r_s)^n/(r_s/r_p)^n=(r_p/r_s)^{2n}$ times larger than that of the final solution. For example, the ratio $(r_p/r_s)^{2n}$ becomes 10^{12} at $n=8,000$ when the deformation at a depth of 10 km ($r_p=6361$ km) due to a source at a depth of 20 km ($r_s=6351$ km) is considered. We confirmed that LSD occurs around $n=8,000$ in actual computation.

In the method using the reciprocity theorem, we obtain (a) the solutions x_1 at the radius r_s caused by external sources such as tide and (b) a solution x_2 that has a unit jump at the radius r_p . They are easily calculated by numerical integration. (c) Finally, the final solution is obtained by multiplying x_1 and x_2 together. This means that we can avoid the LSD that occurs in doing addition.

Keywords: co-seismic deformation, internal deformation, spherically symmetric earth, reciprocity theorem

A change of the crustal vertical ground deformation estimated from the repetition observation of a leveling

*Kazutomo Takano¹

1.GSI of Japan

The Geospatial Information Authority of Japan (GSI) is carrying out the repetition observation of a leveling in the Tokai region from Morimachi to Omaezaki. In the present study, I conducted the examination from the observation of the leveling about the anomalous vertical ground deformation considered to have generated in this region around 2000 to 2005.

Keywords: leveling, crustal vertical deformation, Tokai region

Vertical Deformation Detected by the Precise Levelling Survey in the Periods of Before and After the 2014 Mt. Ontake Eruption and Their Interpretations (2006-2015)

*Masayuki Murase¹, Fumiaki Kimata², Yoshiko Yamanaka³, Shinichiro Horikawa³, Kenjiro Matsuhira³, Takeshi Matsushima⁴, Hitoshi, Y. Mori⁵, Shin Yoshikawa⁶, Rikio Miyajima², Hiroyuki Inoue⁶, Kazunari Uchida⁴, Keigo Yamamoto⁷, Takahiro Ohkura⁶, Manami Nakamoto⁴, Masahiro Yoshimoto³, Takashi OKUDA³, Taketoshi Mishima⁶, Tadaomi Sonoda⁷, Shintaro Komatsu⁷, Kaito Katano¹, Keiji Ikeda⁸, Hiroaki Yanagisawa⁸, Shigeru Watanabe⁸, Haruhisa Nakamichi⁷

1.Department of Earth and Environmental Sciences, College of Humanities and Sciences, NIHON University, 2.Tono Research Institute of Earthquake Science, Association for the Development of Earthquake Prediction, 3.Research Center for Seismology Volcanology and Disaster Mitigation, Graduate School of Environmental Studies, Nagoya University, 4.Institute of Seismology and Volcanology, Faculty of Sciences, Kyushu University, 5.Institute of Seismology and Volcanology, Graduate School of Science, Hokkaido University, 6.Aso Volcanological Laboratory, Graduate School of Science, Kyoto University, 7.Sakurajima Volcano Research Center, Disaster Prevention Research Institute, Kyoto University, 8.Japan Meteorological Agency

We conducted the precise leveling survey in Ontake volcano in April 2015 and discussed vertical deformations detected in the Periods of Before and After the 2014 Mt. Ontake Eruption (2006-2015). Notable uplift (2006-2009) and subsidence (2009-2014) were detected on the eastern flank of the volcano. We estimated pressure source models based on the vertical deformation and used these to infer preparatory process preceding the 2014 eruption. Our results suggest that the subsidence experienced between 2009 and 2014 (including the period of the 2014 eruption) occurred as a result of a sill-like tensile crack with a depth of 2.5 km. This tensile crack might inflate prior to the eruption and deflate during the 2014 activity. A two-tensile-crack model was used to explain uplift from 2006 to 2009. The geometry of the shallow crack was assumed to be the same as the sill-like tensile crack. The deep crack was estimated to be 2 km in length, 4.5 km in width, and 3 km in depth. Distinct uplifts began on the volcano flanks in 2006 and were followed by seismic activities and a small phreatic eruption in 2007. From the partially surveyed leveling data in August 2013, uplift might continue until August 2013 without seismic activity in the summit area. Based on the uplift from 2006 to 2013, magma ascended rapidly beneath the summit area in December 2006, and deep and shallow tensile cracks were expanded between 2006 and 2013. The presence of expanded cracks between 2007 and 2013 has not been inferred by previous studies. A phreatic eruption occurred on 27 September 2014, and, following this activity, the shallow crack may have deflated. In the period between October 2014 and April 2015, small uplift less than 4mm was detected.

Keywords: Ontake volcano, precise leveling survey, deformation

Opening crack associated with the 2015 eruption of the Hakone volcano estimated from InSAR

*Ryosuke Doke¹, Masatake Harada¹, Ryou Honda¹, Yohei Yukutake¹, Kazutaka Mannen¹, Jun Takenaka¹

1. Hot Springs Research Institute of Kanagawa Prefecture

Seismic activities on the Hakone Volcano, which located western part of Kanagawa Prefecture, Japan, were activated from the end of April, 2015. Then, small phreatic eruptions occurred at the Owakudani from 29th June. From the InSAR analysis by using ALOS-2/PALSAR-2 data, we detected a crustal deformation which caused by an opening crack formed during the eruption. Based on the inversion modeling of InSAR data, we defined the geometric and kinematic characteristics of the opening crack.

Estimated crack is trending NW-SE direction and dipping 82.2°NE, with 1.3 km in length and 0.3 km in width. Opening displacement was estimated to be 14.5 cm in a rectangular model. The opening distribution was estimated through the linear inversion, under the condition that the position and orientation of crack were fixed. The result showed that two peaks of opening were in the central shallow part and southern part. Volume changes of the crack were estimated $5.6 \times 10^4 \text{ m}^3$ in the rectangular model and $6.6 \times 10^4 \text{ m}^3$ in the linear model. It is considered that the intrusion of hot water or steam to the crack excited the swelling and triggered the eruption at Owakudani.

Keywords: Hakone Volcano, 2015 phreatic eruption, InSAR, Opening crack, Modeling

Rainfall correction of the Extensometer at Matsushiro

*Kazuhiro Kimura¹, Akio Kobayashi¹, Minoru Funakoshi²

1.Meteorological Research Institute, 2.Matsushiro Seismological Observatory, Earthquake and Tsunami Observation Division, Seismological and Volcanological Department, Japan Meteorological Agency

Japan Meteorological Agency (JMA) installed the quartz tube extensometer of 100m in the tunnel at Matsushiro (Nagano city, Japan). This extensometer data is stable for several decades, but is influenced by the rainfall. Nishimae and Wakui (1996) tried the rainfall correction using a tank model for N-S component of this extensometer. They successfully estimated parameters of the model by trial and error.

We estimate parameters of the tank model by Shuffled Complex Evolution method developed at the University of Arizona (SCE-UA method). The parameters estimated are similar each other.

In addition, we introduce the rainfall correction by the tank model of E-W component of this extensometer.

Keywords: Extensometer, rainfall correction, shuffled complex evolution method developed at the university of arizona

Morphometric evaluation of tectonic activity in the northern Ochigata fault zone in the Southern Noto Peninsula, north-central Japan

*Hiroyuki Yamaguchi¹, Akira Takeuchi²

1.Graduate School of Science and Engineering for Education, University of Toyama, 2.Graduate School of Science and Engineering for Research, University of Toyama

The Ochigata fault zone consists of a 44 km long active faults in a NE-SW direction, from the northern edge to the western part of the Hodatsu hill in the neck of Noto Peninsula, Ishikawa Prefecture. The fault zone is divided into five segments from north to south: the Sekidosan fault, the Furuko fault, the Nodera fault, the Tsuboyama-Hachino fault and the fault of near Uchitakamatsu. The Sekidosan, the northern Nodera and the Uchitakamatsu faults are reverse in slip sense dipping to the east. The southern Nodera and the Tsuboyama-Hachino fault are reverse faults dipping to the west. Their latest event and recurrence interval are revealed by trench investigations performed at the central Sekidosan fault, and pointed out that the uplifting was finished before the Middle Pleistocene based of the geologic structure. However, the pattern of tectonic activity through the fault zone is unclear.

This study examined tectonic deformation of the northern Ochigata fault zone using Mountain-front sinuosity (S_{mf}) and the ratio of valley floor width to valley height (V_f), which were morphometric indices for representing tectonic activity. S_{mf} is explained as the ratio of length of mountain front along the foot of mountain to the straight length of mountain front. The poorer development of sinuosity means the higher uplift rates, and is consistent with the lower value of S_{mf} . V_f is explained by the ratio of width of valley floor to relative elevation between ridge and valley floor. In an area with high uplift rates, topographic profile illustrates a V-shaped profile with the both lower values. This study calculated the value of V_f at a position of 200 m on the mountain side from mountain front. In our morphometric analysis, the 5m-DEM of the Geospatial Information Authority of Japan publication was utilized, and was combined with the slope map and the over ground openness map for interpreting geomorphology of the mountain front.

Separating the mountain front of Sekidosan fault into 22 sections and the northern Nodera fault into 3 sections, the values of S_{mf} within the Sekidosan fault ranged from 3 to 6 at the northern part, 2 to 3.5 at the central and 4 to 25 at the southern. The values of S_{mf} at the northern Nodera fault were 3.5 to 11. The values of V_f within the Sekidosan fault were 2 to 6 at the northern part, 0.5 to 3 at the central and 4 to 35 at the southern. The values of V_f at the northern Nodera fault ranged from 4 to 6. The both indices for the Sekidosan fault performed lower at the center part, and the values of the northern and southern parts of Sekidosan fault and those of the northern Nodera fault became higher. In other words, tectonic activity of the northern Ochigata fault zone is the highest at the central Sekidosan fault and the activity tend to decrease towards the both terminations of Sekidosan fault and the northern Nodera fault.

No case study on S_{mf} and V_f has ever been done in Japan. To examine the quantitative relationship between the two indices and uplift rates, it is important to accumulate the more geological and geomorphological data.

Keywords: morphometric analysis, tectonic activity, Ochigata fault zone